Hybrid Laser Cavity Design for Improved Photon Lifetime and Performance

Yash Mehta, Kun-Chieh Chien, Lei Lei, Kenan Gundogdu, Chih-Hao Chang, and Franky So, *Fellow, IEEE*

***Abstract*— We report an optical cavity design that combines a distributed feedback (DFB) cavity as the primary feedback element for lasing with a silver mirror acting as a Fabry-Pérot cavity for broadband reflection and mode confinement. To evaluate the design, we studied the effects of the silver mirror by excluding the DFB cavity and compared its amplified spontaneous emission (ASE) properties with the sample without the mirror. In the structure with the mirror, the gain medium undergoes ASE at an excitation fluence of 17.5 $\mu J cm^{-2}$ compared to 37 $\mu J cm^{-2}$ for the sample without the mirror. This lower ASE threshold is attributed to enhanced mode confinement and photon density of states (PDOS) from the silver mirror increasing the cavity photon lifetime (τ_c). Using this hybrid cavity, a multimode optically pumped laser with a threshold of 42 $\mu J cm^{-2}$ is demonstrated. This hybrid cavity design offers an effective solution that can be readily applied to other thin film-based laser devices.**

***Index Terms*— Metal halide perovskites, amplified spontaneous emission (ASE), cavity photon lifetime.**

I. Introduction

HYBRID organic-inorganic halide perovskites have emerged as a potential candidate for laser applications due to their facile solution processing, narrow emission linewidth and tunability spanning the visible spectrum [1]. Specifically, due to their cascading energy bands, quasi-2D Ruddlesden-Popper perovskites ($A'_2A_{n-1}B_nX_{3n+1}$) are a suitable class of materials for laser applications. These quantum wells are defined by the inorganic $[PbX_6]^{4-}$ octahedral cage surrounded by a dielectric barrier formed by the bulky A′ site organic cations while the A cations occupy the space between corner-sharing octahedra. The bandgap is determined by the number of adjoining octahedral layers n [2]. The appeal of quasi-2D perovskites is that the exciton generated in the large bandgap domains can funnel through the energy staircase to the lower bandgap domain ($n \approx \infty$) where they accumulate with longer excited-state lifetimes, resulting in high radiative recombination efficiency required for lasing [3].

Manuscript received 2 December 2023; revised 30 January 2024; accepted 28 February 2024. Date of publication 8 March 2024; date of current version 13 March 2024. This work was supported by NSF Designing Materials to Revolutionize and Engineer our Future (DMREF) Program under Contract 2323802. *(Corresponding author: Franky So.)*

Yash Mehta, Lei Lei, and Franky So are with the Department of Material Science and Engineering, North Carolina State University, Raleigh, NC 27695 USA (e-mail: ymehta@ncsu.edu; llei2@ncsu.edu; fso@ncsu.edu).

Kun-Chieh Chien and Chih-Hao Chang are with the Walker Department of Mechanical Engineering, The University of Texas at Austin, Austin, TX 78712 USA (e-mail: kc.chien@utexas.edu; chichang@utexas.edu).

Kenan Gundogdu is with the Department of Physics, North Carolina State University, Raleigh, NC 27695 USA (e-mail: kgundog@ncsu.edu).

Color versions of one or more figures in this letter are available at https://doi.org/10.1109/LPT.2024.3374261.

Digital Object Identifier 10.1109/LPT.2024.3374261

In an optical cavity, the Purcell factor (F_p) quantifies the modified decay rate of a dipole placed inside the cavity through the relation $F_p \propto Q/V$, where Q is the quality factor and V is the mode volume. A high Purcell factor leads to a faster decay, and consequently to a narrower emission linewidth [4]. Thus, by adjusting the Purcell factor it is possible to manipulate the radiation lifetime, which is crucial for attaining population inversion and lasing. A high Purcell factor requires a cavity with a large quality factor and a high mode confinement (small V).One way to increase the mode confinement is to use metallic mirrors as they offer enhanced mode confinement (Γ) by suppressing mode penetration in comparison to dielectric mirrors. This leads to a reduced mode volume (V) and consequently, a higher Purcell factor [5], [6]. However, using metallic mirrors within a cavity also has some drawbacks. First, it can result in lossy coupling between the optical modes and the Surface Plasmon Polariton (SPP) mode at the metal interface. Second, the presence of a metallic mirror causes notable Joule loss due to radiation absorption and consequently gives rise to non-radiative decay [7].

To circumvent these issues, we propose a 'hybrid' cavity design that combines a DFB cavity with a Fabry-Pérot cavity formed by a planar metallic mirror as pictured in *Fig. 1(a)*. The DFB cavity provides the primary feedback for oscillations while the vertical Fabry-Pérot cavity confines the optical mode volume. To suppress emission quenching, the gain media is separated from the silver mirror with a dielectric interlayer which also acts as a buffer layer for nanoimprinting the DFB grating. Subsequently, we show that the ASE threshold is reduced by a factor of 2 compared to perovskite-on-glass, indicating a high level of gain efficiency. It should be noted our hybrid cavity design applies to other gain materials. Finally, we demonstrate a multi-mode laser based on this hybrid structure showcasing the characteristics of both DFB and Fabry-Pérot cavity that exhibit long photon lifetime and therefore low operational threshold.

II. Experimental Results and Discussion

Lasing in a gain medium is generally supported by trapped waveguided modes in the film. For a non-leaky waveguide mode to be supported, the film must have a minimum thickness of $\lambda/2n_{eff}$, where n_{eff} is the effective refractive index of a mode propagating through the material with a wavevector $\vec{k} = 2\pi/\lambda$. The presence of these trapped modes facilitates population inversion, a prerequisite for stimulated emission [8]. To understand how the trapped mode affects lasing, we study the effect of confinement on the modal gain G_m. Modal gain is related to the intrinsic material gain $G_a$by the relation $G_m = \Gamma G_a$ where Γ is the confinement factor [9]. With an increase in the mode confinement, the overall modal gain can exceed the material gain resulting in improved light amplification. To ensure maximum mode confinement factor for a planar perovskite film, we optimized the spin-coating process to yield a smooth 80 ± 10 nm thick film. A film thickness greater than that results in rough surface morphology [10] and supports higher-order leaky waveguided modes reducing the mode utilization efficiency (*Fig. S1*) [11]. As shown in *Figs. 1(a-b)*, negligible waveguide mode contribution results from weak confinement and therefore low reflectance at the surrounding interfaces causing mode leakage.Therefore, to enhance the mode confinement we introduce a thin silver film between the glass substrate and the perovskite layer for which the waveguide mode contribution increases to almost 70% [12].

However, the inclusion of the silver reflector directly below the perovskite layer introduces losses due to the presence of the surface plasmons [13]. As the SPP mode propagates along the metal-dielectric interface it either gets scattered or is absorbed by the metal and dissipated as heat. These losses are determined by the distance separating the emitter and the silver film. SPP mode is dominant for an 80 ± 10 nm thick perovskite film in direct contact with the silver. To mitigate this loss channel, a dielectric interlayer is introduced between the perovskite and the silver reflector to physically separate them thereby reducing the coupling to the metal's surface plasmon. For an interlayer thickness greater than 20 nm, the SPP mode contribution drops rapidly, meanwhile the waveguide mode increases and remains almost constant irrespective of interlayer thickness (*Fig. 1(a)*) [14]. Additionally, the interlayer serves as a buffer layer onto which a one-dimensional DFB grating is nanoimprinted (SI).

Apart from the film thickness, the index contrast must be high at the interfaces surrounding the gain medium to suppress mode leakage and subsequently increase the mode contribution. From *Fig. 1(b)*, the perovskite-air interface has a reflectance value of 0.37 at 530 nm and is unmodified to facilitate a pathway for optical excitation of the gain medium. For the perovskite-glass interface, the reflectance is only about 0.27 which causes severe mode leakage, but with the introduction of a silver layer the reflectance is significantly improved. The oscillations in the reflectance spectrum is due to the cavity effect resulting from different phase conditions. However, the strength of the cavity effect diminishes as the silver film thickness is increased.

Unlike nanostructured patterns, planar metallic mirror does not modify the magnitude of the wavevector, however, it also does not distinguish between the wavevectors of the modes that provide constructive feedback and the ones that do not. This is undesirable because a frequency-selective cavity can effectively filter out unwanted regions of the emission spectrum that do not contribute to light amplification and can be detrimental to the spatial coherence of the resulting laser emission [15]. Hence, to achieve an optimal balance between high reflectance and a strong cavity effect a 30 nm thick silver film is used. For this thickness, the interface reflectance increases to

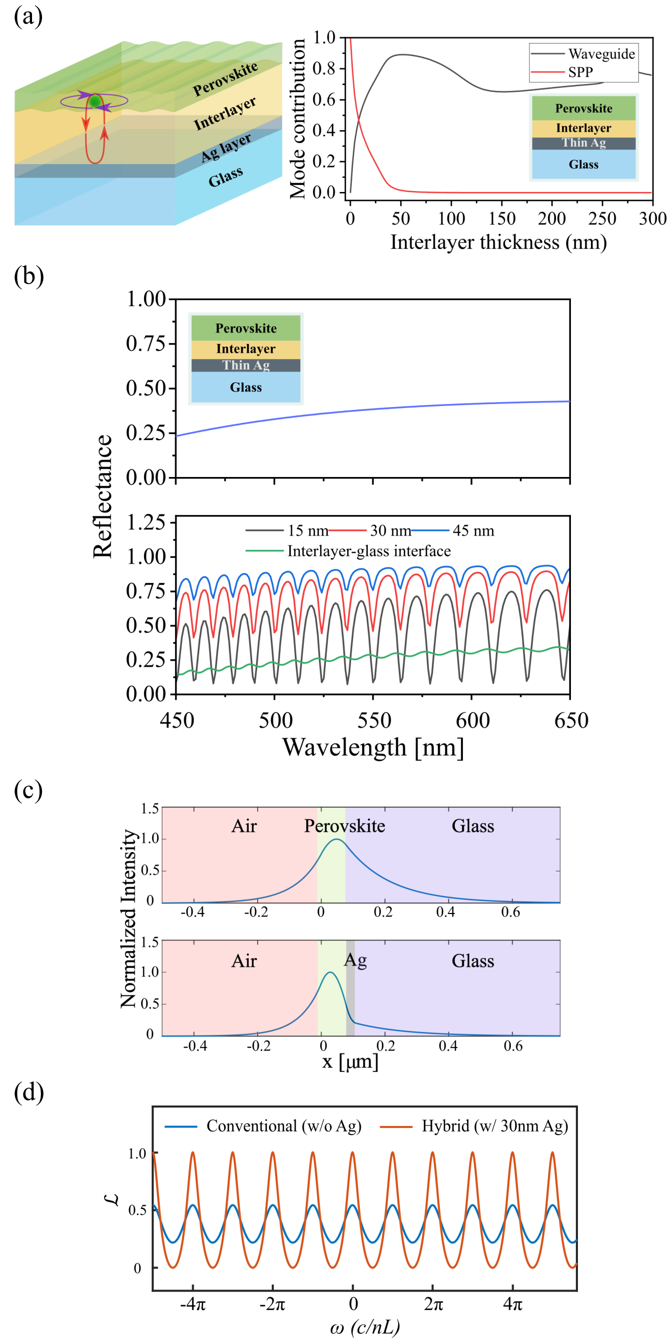

Fig. 1. (a) Hybrid device structure with DFB and Fabry-Pérot elements; SPP and waveguide mode as a function of the interlayer thickness. (b) top panel-reflectance at the perovskite-air interface, bottom panel-reflectance at the interlayer-Ag interface for different thicknesses. (c) TE0 field distribution in the presence of the Ag layer causes improved mode confinement. (d) Comparing the transmittance function for the case of with and without Ag.

0.84 leading to strong mode confinement (*Fig.1(c)*) and hence a larger PDOS which eventually enhances the Purcell factor [16].

Stimulated emission is dependent on PDOS [17], and hence an augmented PDOS facilitates population inversion. Therefore, to indirectly probe this effect we analyzed the modified local photon density of states (LPDOS) due to the silver reflector with respect to the free space PDOS according to the expression,

$$\rho_{cav}(\omega_k, k) = \rho_{free}\mathcal{L}(\omega_k) \tag{1}$$

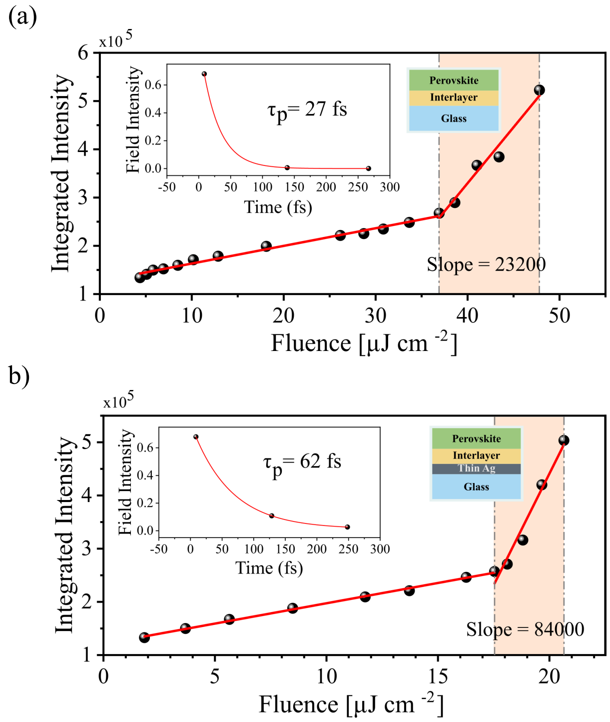

Fig. 2. Intensity vs fluence curve highlighting the ASE regime (shaded) for **(a)** without Ag: threshold fluence of $36.9\mu J/cm^2$ and **(b)** with Ag: threshold of $17.5\mu J/cm^2$. Inset: FDTD simulation results for τ_c [18].

where $\mathcal{L}(\omega_k)$ is the cavity transmission, and is given by [9],

$$\mathcal{L}(\omega_k) = \frac{1}{1 + \frac{4\mathcal{F}^2}{\pi^2}\sin^2\left(\frac{\omega_k n L}{c}\right)} \tag{2}$$

where $\mathcal{L}$ is the cavity length, $\mathcal{F} = \pi\,(R_1 R_2)^{0.25}/(1-\sqrt{R_1 R_2})$ is the cavity finesse, R_1 and R_2 are the reflectance at the perovskite-air and the interlayer-metal interface respectively. A plot of the normalized transmission peak for the device with silver mirror is compared to the conventional case in *Fig. 1(d)*, taking into consideration the numeric values of the film thickness and reflectance as defined above. By incorporating a silver mirror, the interference pattern is pronounced while maintaining the spectral characteristics which indicates an enhanced optical filtering capability. Because of increased cavity transmission, the LPDOS is enhanced, which can be experimentally verified from the photoluminescence (PL) emission as a function of the silver layer thickness in *Fig. S2* along with the superimposed Fabry-Pérot oscillation.

The modified gain properties of the film can be obtained from the amplified spontaneous emission (ASE) measurements as it propagates through an inverted medium without any feedback. In *Figs. 2(a-b),* the output light intensity vs. excitation fluence curve for a perovskite film on a glass substrate (conventional structure) is compared to the one with a silver reflector. In both configurations at low external pumping power, the integrated intensity of the spontaneous emission peak at 525 nm exhibits a linear progression until it reaches a certain threshold fluence beyond which, the curve demonstrates a noticeably steeper slope due to the ASE peak at 533 nm. The slope of this region, called slope efficiency, is used to assess the photon lifetimes and the effectiveness of the amplification process [19]. The slope efficiency of the device with a silver layer is 3.6 times higher with a lower threshold fluence of 17.5 μJcm^{-2} than that of the device without a silver reflector having a threshold of 36.9 μJcm^{-2}. This suggests an enhanced photon lifetime and is consistent with the enhanced LPDOS [20]. A high slope efficiency with a low operational threshold implies that an overall higher laser throughput can be achieved for the same gain medium and external pumping scheme.

To confirm the enhancement in the cavity photon lifetime, a Finite Difference Time Domain (FDTD) simulation was performed where a time monitor records the photon wave packet's intensity as a function of time while undergoing back-and-forth reflections at the interfaces surrounding the gain medium. From the inset in *Figs. 2(a-b)*, the light intensity takes 27 fs and 62 fs to decay in the structure without and with the silver layer respectively. The observed 2.3-times enhancement in photon lifetime provides further evidence that photons have a prolonged existence within the structure with the silver mirror compared to the conventional structure which subsequently assists with light amplification.

Finally, we fabricated a hybrid lasing structure incorporating DFB cavity, serving as the primary feedback element with the silver reflector. To determine the optimum grating pitch for the 2nd order DFB cavity we performed angle-resolved photoluminescence (ARPL) measurements to ensure resonance along the normal direction [21]. According to the Bragg's law $\vec{k}' = \vec{k} \pm m\vec{k}_G$, where $\vec{k}_G = 2\pi/\Lambda$ is the grating wavevector implying that the cavity resonance can be tuned through Λ. From the ARPL results in *Fig. 3(a)*, we found that a grating pitch of $\Lambda = 295\pm5$nm results in a strong intensity modulation in the normal direction.

Equally spaced oscillatory modes superimposed on the PL spectra were observed (*Fig. 3(b)*) for a fluence of 21.6 μJcm^{-2} which is characteristic of the Fabry-Pérot etalon [22]. From the Free Spectral Range (FSR) given by $\Delta\lambda = \lambda^2/2n_{eff}l$, effective mode index ($n_{eff}$) can be evaluated for a cavity length l. For $l \approx 21$ μm consisting of perovskite and the interlayer combined, λ =533 nm, $\Delta\lambda = 3.6$ nm, we get $n_{eff} = 1.87$ which agrees well with the TE0 mode index from FDTD simulation (n_{eff}^{FDTD} =1.88). This implies that the mode is predominantly trapped inside the perovskite and the additional modes due to the interlayer have negligible contributions to lasing. It is worth mentioning that the silver mirror interacts strongly only with the 2nd order wavevector from the DFB grating due to its transverse nature leaving the oscillating 1st order mode unperturbed.

As seen from the lasing spectrum in *Fig. 3(b)*, the transverse dimensions of the cavity result in closely spaced Fabry-Pérot modes with a separation of only 5 nm. Due to this close spacing, several cavity modes coexist within the gain bandwidth of perovskite causing multi-mode lasing at a threshold of 42 μJcm^{-2}. The stimulated emission peak comprises of 3 modes (inset of *Fig. 3(b)*) which exhibits linear increase while the other modes remain pinned. From *Fig. 3(a),*the integrated intensity shows a characteristic lasing curve with a sudden increase in the output light intensity at the threshold fluence supplemented by a decrease in the linewidth followed

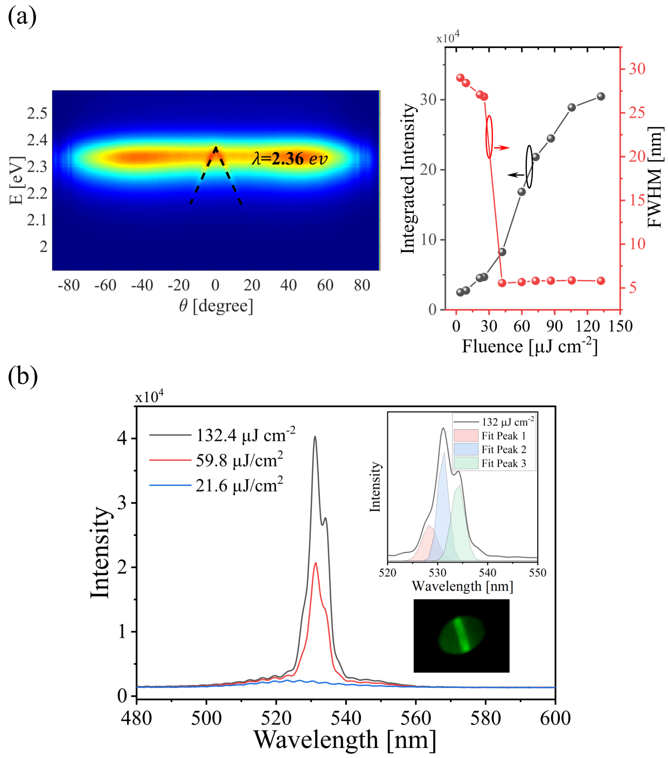

Fig. 3. (a) ARPL for $\Lambda = 295nm$ grating. The input-output laser light curve; along with the FWHM as a function of the excitation fluence. **(b)** Multimode lasing behavior with the inset showing the composite linewidth, and a photograph of a central bright fringe typical of lasing behavior.

by a regime of gain saturation at higher excitation. The FWHM of the composite curve is 4.8 nm with individual modes having a width of 2.4 nm. As added proof for lasing, a central bright fringe is observed in the far-field emission (*Fig. 3(b) inset*), however, due to the multimode lasing behavior the spatial coherence is low causing beam divergence [8].

III. Conclusion

In this work, we combined a distributed feedback (DFB) cavity and Fabry-Pérot etalon to create a hybrid optical cavity. The inclusion of the metal reflector at the bottom interface reduces the mode volume leading to an improved Purcell factor. The increased interface reflectance also facilitates an extended photon interaction time with the perovskite gain media and augments the local photon density of states. The photon lifetime is enhanced by a factor of ~2.5 resulting in an improved slope efficiency and a decreased threshold for the onset of amplification. Although the lasing linewidth is not as narrow as single-mode perovskite laser, such multimode lasers still have a relatively narrowband compared to incoherent light sources making them useful in applications where intermediate spatial coherence is required [23].

References

[1] A. Zanetta et al., "Manipulating color emission in 2D hybrid perovskites by fine tuning halide segregation: A transparent green emitter," *Adv. Mater.*, vol. 34, no. 1, Jan. 2022, Art. no. 2105942, doi: 10.1002/adma.202105942.

[2] C. C. Stoumpos et al., "Ruddlesden–popper hybrid lead iodide perovskite 2D homologous semiconductors," *Chem. Mater.*, vol. 28, no. 8, pp. 2852–2867, Apr. 2016, doi: 10.1021/acs.chemmater.6b00847.

[3] L. Lei et al., "Efficient energy funneling in quasi-2D perovskites: From light emission to lasing," *Adv. Mater.*, vol. 32, no. 16, Apr. 2020, Art. no. 1906571, doi: 10.1002/adma.201906571.

[4] B. Romeira and A. Fiore, "Purcell effect in the stimulated and spontaneous emission rates of nanoscale semiconductor lasers," *IEEE J. Quantum Electron.*, vol. 54, no. 2, pp. 1–12, Apr. 2018, doi: 10.1109/JQE.2018.2802464.

[5] S. Kéna-Cohen, S. A. Maier, and D. D. C. Bradley, "Ultrastrongly coupled exciton-polaritons in metal-clad organic semiconductor microcavities," *Adv. Opt. Mater.*, vol. 1, no. 11, pp. 827–833, Nov. 2013, doi: 10.1002/adom.201300256.

[6] Y. Jia, R. A. Kerner, A. J. Grede, A. N. Brigeman, B. P. Rand, and N. C. Giebink, "Diode-pumped organo-lead halide perovskite lasing in a metal-clad distributed feedback resonator," *Nano Lett.*, vol. 16, no. 7, pp. 4624–4629, Jul. 2016, doi: 10.1021/acs.nanolett.6b01946.

[7] K. Ding and C. Z. Ning, "Metallic subwavelength-cavity semiconductor nanolasers," *Light, Sci. Appl.*, vol. 1, no. 7, p. e20, Jul. 2012, doi: 10.1038/lsa.2012.20.

[8] A. E. Siegman, *Lasers*. Taiwan: Univ. Science, 1986.

[9] L. A. Coldren, S. W. Corzine, and M. L. Mashanovitch, *Diode Lasers and Photonic Integrated Circuits*. Hoboken, NJ, USA: Wiley, 2012.

[10] L. Qin et al., "Enhanced amplified spontaneous emission from morphology-controlled organic–inorganic halide perovskite films," *RSC Adv.*, vol. 5, no. 125, pp. 103674–103679, 2015, doi: 10.1039/c5ra20167e.

[11] T. S. Misirpashaev and C. W. J. Beenakker, "Lasing threshold and mode competition in chaotic cavities," *Phys. Rev. A, Gen. Phys.*, vol. 57, no. 3, pp. 2041–2045, Mar. 1998, doi: 10.1103/physreva.57.2041.

[12] N. Tessler, "Lasers based on semiconducting organic materials," *Adv. Mater.*, vol. 11, no. 5, pp. 363–370, Mar. 1999, doi: 10.1002/(SICI)1521-4095(199903)11:5<363::AID-ADMA363>3.0.CO;2-Y.

[13] P. Berini and I. De Leon, "Surface plasmon–polariton amplifiers and lasers," *Nature Photon.*, vol. 6, no. 1, pp. 16–24, Jan. 2012, doi: 10.1038/nphoton.2011.285.

[14] T. P. A. van der Pol, K. Datta, M. M. Wienk, and R. A. J. Janssen, "The intrinsic photoluminescence spectrum of perovskite films," *Adv. Opt. Mater.*, vol. 10, no. 8, Apr. 2022, Art. no. 2102557, doi: 10.1002/adom.202102557.

[15] W. E. Hayenga and M. Khajavikhan, "Unveiling the physics of microcavity lasers," *Light, Sci. Appl.*, vol. 6, no. 8, p. 17091, Aug. 2017, doi: 10.1038/lsa.2017.91.

[16] H. Yokoyama, "Physics and device applications of optical microcavities," *Science*, vol. 256, no. 5053, pp. 66–70, Apr. 1992, doi: 10.1126/science.256.5053.66.

[17] H. Haug, "Quantum-mechanical rate equations for semiconductor lasers," *Phys. Rev.*, vol. 184, no. 2, pp. 338–348, Aug. 1969, doi: 10.1103/physrev.184.338.

[18] G. Berden, R. Peeters, and G. Meijer, "Cavity ring-down spectroscopy: Experimental schemes and applications," *Int. Rev. Phys. Chem.*, vol. 19, no. 4, pp. 565–607, Oct. 2000, doi: 10.1080/014423500750040627.

[19] S. Zeng, X. Zhao, Y. Zhu, C. Dove, and L. Zhu, "Slope efficiency of integrated external cavity hybrid lasers: A general model and analysis," *AIP Adv.*, vol. 9, no. 3, Mar. 2019, Art. no. 035201, doi: 10.1063/1.5078636.

[20] A. Muravitskaya et al., "Engineering of the photon local density of states: Strong inhibition of spontaneous emission near the resonant and high-refractive index dielectric nano-objects," *J. Phys. Chem. C*, vol. 126, no. 12, pp. 5691–5700, Mar. 2022, doi: 10.1021/acs.jpcc.1c09844.

[21] X. Fu et al., "Mode dispersion in photonic crystal organic light-emitting diodes," *ACS Appl. Electron. Mater.*, vol. 2, no. 6, pp. 1759–1767, Jun. 2020, doi: 10.1021/acsaelm.0c00326.

[22] Y. Mi et al., "Fabry–Pérot oscillation and room temperature lasing in perovskite cube-corner pyramid cavities," *Small*, vol. 14, no. 9, Mar. 2018, Art. no. 1703136, doi: 10.1002/smll.201703136.

[23] A. Ahmad, N. Jayakumar, and B. S. Ahluwalia, "Demystifying speckle field interference microscopy," *Sci. Rep.*, vol. 12, no. 1, p. 10869, Jun. 2022, doi: 10.1038/s41598-022-14739-0.